Crystal Structure of Flavocetin-A, a Platelet Glycoprotein Ib-Binding Protein, Reveals a Novel Cyclic Tetramer of C-Type Lectin-like Heterodimers[†,‡]

Kouichi Fukuda,[§] Hiroshi Mizuno,*[,§,||] Hideko Atoda,[⊥] and Takashi Morita[⊥]

Institute of Applied Biochemistry, University of Tsukuba, Tsukuba, Ibaraki 305-8572, Japan, Department of Biotechnology, National Institute of Agrobiological Resources, Tsukuba, Ibaraki 305-8602, Japan, and Department of Biochemistry, Meiji Pharmaceutical University, Kiyose, Tokyo 204-8588, Japan

Received September 14, 1999; Revised Manuscript Received December 13, 1999

ABSTRACT: Snake venom contains a number of the hemostatically active C-type lectin-like proteins, which affect the interaction between von Willebrand factor (vWF) and the platelet glycoprotein (GP) Ib or platelet receptor to inhibit/induce platelet activation. Flavocetin-A (FL-A) is a high-molecular mass C-type lectin-like protein (149 kDa) isolated from the habu snake venom. FL-A binds with high affinity to the platelet GP Ibα-subunit and functions as a strong inhibitor of vWF-dependent platelet aggregation. We have determined the X-ray crystal structure of FL-A and refined to 2.5 Å resolution. This is a first elucidation of a three-dimensional structure of the platelet GP Ib-binding protein. The overall structure reveals that the molecule is a novel cyclic tetramer $(\alpha\beta)_4$ made up of four $\alpha\beta$-heterodimers related by a crystallographic 4-fold symmetry. The tetramerization is mediated by an interchain disulfide bridge between cysteine residues at the C-terminus of the α-subunit and at the N-terminus of the β-subunit in the neighboring $\alpha\beta$-heterodimer. The high affinity of FL-A for the platelet GP Ib α-subunit could be explained by a cooperative-binding action through the multiple binding sites of the tetramer.

Glycoprotein (GP)[1] Ib is an important platelet adhesion receptor and plays an essential role in primary hemostasis (reviewed in *1*, *2*). Adhesion of platelets to sites of vascular injury is initiated by the interaction of von Willebrand factor (vWF) exposed on the subendothelium with the platelet GP Ib (*3*, *4*). The same interaction also precipitates pathological platelet aggregation induced by high shear stresses, which occurs at sites of arterial stenosis (*5*−*7*).

A number of the hemostatically active proteins that affect the interaction between vWF and the platelet GP Ib have been isolated from the venom of several snake species and characterized (reviewed in *8*). The venom proteins, which modulate the vWF−GP Ib interaction, have several implications for the elucidation of biological mechanism underlying hemostasis. Botrocetin is a platelet agglutination inducer from the *Bothrops jararaca* venom (*9*−*12*). It is a disulfide-linked heterodimer protein composed of homologous α- and β-subunits (*13*). This protein binds to vWF to form an active complex, resulting in platelet agglutination (*14*). Sugimoto et al. provided the first evidence for the location of botrocetin-binding sites in the A1 domain of vWF (*15*). Bitiscetin is another platelet agglutination inducer from the *Bitis arietans* venom (*16*). Although bitiscetin is also a disulfide-linked heterodimer composed of homologous α- and β-subunits (*17*), it binds to the A3 but not to the A1 domain (*18*). On the other hand, many GP Ib-binding (but not vWF-binding) proteins have been purified from the venom of several snake species (*19*−*26*) and sequenced (*25*−*30*). Most of them are known to inhibit vWF-dependent platelet aggregation, whereas they are heterodimers similar to botrocetin (reviewed in *31*), and low-molecular mass proteins (∼30 kDa) belonging to the C-type lectin superfamily (*32*).

Recently, a high-molecular mass GP Ib-binding protein was isolated from the habu snake *Trimeresurus flavoviridis* venom (*33*). This protein, called flavocetin-A (FL-A), has a molecular mass of 149 kDa under nonreducing condition. On reduction, FL-A showed two subunits α (17 kDa) and β (14 kDa). The amino acid sequences of both subunits of FL-A have been recently determined.[2] Sequence comparison revealed that each subunit showed high sequence identity to the corresponding subunit of the low-molecular mass GP Ib-binding proteins. Among those proteins, FL-A binds with the highest affinity ($K_d = 0.35 \pm 0.13$ nM) to the platelet GP Ib and strongly inhibits vWF-dependent aggregation of fixed human platelets and also inhibits shear-induced platelet aggregation at high shear stress (*33*). To understand this

[†] This work was in part supported by Special Coordination Funds for Promoting Science and Technology of STA to H. M. and by a Research Grant for Cardiovascular Diseases (8A-1) from the Ministry of Health and Welfare to T. M.

[‡] The atomic coordinates of FL-A are available from the Protein Data Bank, the Research Collaboratory for Structural Bioinformatics (http://www.rcsb.org/pdb/) under entry code 1C3A.

[§] University of Tsukuba.

[||] National Institute of Agrobiological Resources.

[⊥] Meiji Pharmaceutical University.

* To whom correspondence should be addressed. Department of Biotechnology, National Institute of Agrobiological Resources, Tsukuba, Ibaraki 305-8602, Japan. Telephone: +81-298-38-7014. Fax: +81-298-38-7408. E-mail: mizuno@abr.affrc.go.jp.

[1] Abbreviations: GP, glycoprotein; vWF, von Willebrand factor; FL-A, flavocetin-A; IX/X-bp, coagulation factors IX/X-binding protein; rms, root-mean-square; IX-bp, coagulation factor IX-binding protein; Wat, water; CVX, convulxin.

[2] Manuscript in preparation.

10.1021/bi992134z CCC: $19.00
Published on Web 02/22/2000

Table 1: Statistics of Data Collection and Structure Refinement

data collection	
resolution range (Å)	85−2.5 (2.6−2.5)[a]
unique reflections	15 078
multiplicity	6.4
completeness (%)	95.6 (74.2)
R_{merge} (%)	8.2 (38.0)
structure refinement	
resolution range (Å)	6.0−2.5 (2.6−2.5)
number of reflections	
$F_o \geq 2\sigma$	11 391
all data without σ cutoff	13 893
number of non-hydrogen protein atoms	2124
number of water molecules	93
R-factor (%)[b]	
$F_o \geq 2\sigma$	21.0 (32.9)
all data without σ cutoff	23.1 (40.7)
R_{free} (%)[c]	
$F_o \geq 2\sigma$	26.9 (35.4)
all data without σ cutoff	28.6 (39.1)
rms deviations from ideal geometry	
bond lengths (Å)	0.007
bond angles (deg)	1.6
dihedral angles (deg)	23.1
improper angles (deg)	1.0
average *B*-factor (Å^2)	
protein	35.2
solvent	54.7

[a] Numbers in parentheses refer to the values for the outer shell. [b] *R*-factor $= \Sigma||F_o| - |F_c||/\Sigma|F_o|$. [c] R_{free} was calculated with randomly selected 5% of the reflections not used in the refinement.

functional specificity and the molecular recognition of the C-type lectin-like heterodimers, structural studies of FL-A have been initiated.

Here, we report the three-dimensional structure of a high-molecular mass C-type lectin-like protein determined by X-ray crystallography method. The structure is unique in showing a cyclic tetramer $(\alpha\beta)_4$ made up of four identical $\alpha\beta$-heterodimers (hereafter, the heterodimer unit of FL-A is referred to as $\alpha\beta$-heterodimer), which are arranged in a manner of "head-to-tail" interaction, based on a crystallographic 4-fold symmetry. The tetramerization is mediated by an interchain disulfide bridge, newly identified between the $\alpha\beta$-heterodimers. To the best of our knowledge, the structure is the first to be solved among the GP Ib-binding proteins, and it has a unique disulfide-linked oligomer.

EXPERIMENTAL PROCEDURES

Crystallization and Data Collection. FL-A was purified from the venom of *T. flavoviridis* as described previously (*33*) with modification. The crude venom was dissolved in a buffer containing 50 mM Tris-HCl, pH 8.0, and 0.1 M NaCl and applied to a gel filtration column of Sephacryl S-200 HR (Pharmacia). Subsequently, the eluent was chromatographed using Q- and S-Sepharose Fast Flow ion-exchange columns (both from Pharmacia). Prismatic crystals of FL-A were grown at 20 °C from a reservoir solution containing 9% (v/v) 2-methyl-2,4-pentanediol, 0.1 M sodium acetate buffer, pH 4.6, and 10 mM $CaCl_2$ as described previously (*34*). The crystals belong to the tetragonal space group *I* 4 with cell dimensions of $a = b = 120.5$ Å and $c = 62.8$ Å. There is one $\alpha\beta$-heterodimer of FL-A in the asymmetric unit with a solvent content of 67% ($V_m = 3.7$ Å^3/Da). X-ray data collection experiment was performed at room temperature at the beamline BL6B at the synchrotron facility, the Photon Factory in High Energy Accelerator Research Organization, Tsukuba, Japan. X-ray data were collected with the Weissenberg imaging-plate detector system (*35*). The crystal-to-detector distance was 573 mm. The intensity data up to 85−2.5 Å resolution were processed with the programs DENZO and SCALEPACK (*36*).

Molecular Replacement. The structure of FL-A was solved by a molecular replacement method using the program AMoRe (*37*) in the CCP4 suite (*38*). The search probe was a homology-based heterodimer model constructed with the program HOMOLOGY in the package INSIGHT II (Molecular Simulation Inc.) using the sequence of FL-A and the atomic coordinates (PDB code 1IXX) of a homologous protein, coagulation factors IX/X-binding protein (IX/X-bp) from the venom of *T. flavoviridis* (*39*). The N-terminal residues 1−2 and the C-terminal residues 132−135 of the α-subunit and the corresponding residues 1−3 and 123−125 of the β-subunit were then removed. The search model was minimized by the Powell minimization method. A cross-rotation-function search was calculated against all data in the resolution range between 20 and 3.5 Å with a sphere radius of 30 Å and an angular step size of 2.5°. The highest peak from the rotation-function search had a height of 10.8σ, while the next highest peak was at 8.5σ. This rotation-function solution was identified at the Eulerian angles of $\alpha = 84.5°$, $\beta = 47.0°$, and $\gamma = 85.8°$. This orientation revealed a number of peaks up to 4.8σ in the translation-function searches, but one of the peaks with a correlation coefficient of 20.9% and an *R*-factor of 54.7% led to the correlation coefficient of 31.7% after the fast-rigid-body refinement (AMoRe), which is much higher than did other peaks. This translation-function solution was identified at fractional coordinates of $x = 0.9850$, $y = 0.3650$, and $z = 0.0000$. Graphical inspection of this solution using the program QUANTA version 97 (Molecular Simulation Inc.) revealed that the molecule of FL-A is a tetramer made up of four $\alpha\beta$-heterodimers related by a crystallographic 4-fold symmetry parallel to the *c*-axis, and favorable intermolecular interactions.

Structure Refinement. All crystallographic refinements were performed using the program X-PLOR (*40*) and the parameter set of Engh and Huber (*41*). The R_{free} (*42*) was calculated with randomly selected 5% reflections not used in the refinement from the beginning process. The initial model obtained from the molecular replacement procedure was first subjected to a rigid-body refinement, and then a simulated annealing to 3000−300K at 3.0 Å resolution. This resulted in an initial *R* factor of 29.4% and R_{free} of 46.8%. A $2F_o-F_c$ map showed that the β-subunit was correctly modeled, but the α-subunit was required to rotate approximately 10° relative to the β-subunit around the linker region to fit in the electron density. This might be the reason the molecular replacement calculation did not show a clear solution in the translation-function searches. The model was manually adjusted using the program QUANTA on a Silicon Graphics workstation Indigo2 R10000. After the rigid-body refinement, a simulated annealing of this adjusted model was continued, and the *R*-factor and R_{free} dropped to 23.0% and 38.7%, respectively. At this stage, the quality of the $2F_o-F_c$ map was sufficient to find the omitted residues in the N- and C-terminal regions. The entire model was rebuilt and subjected to further refinement using simulated anneal-

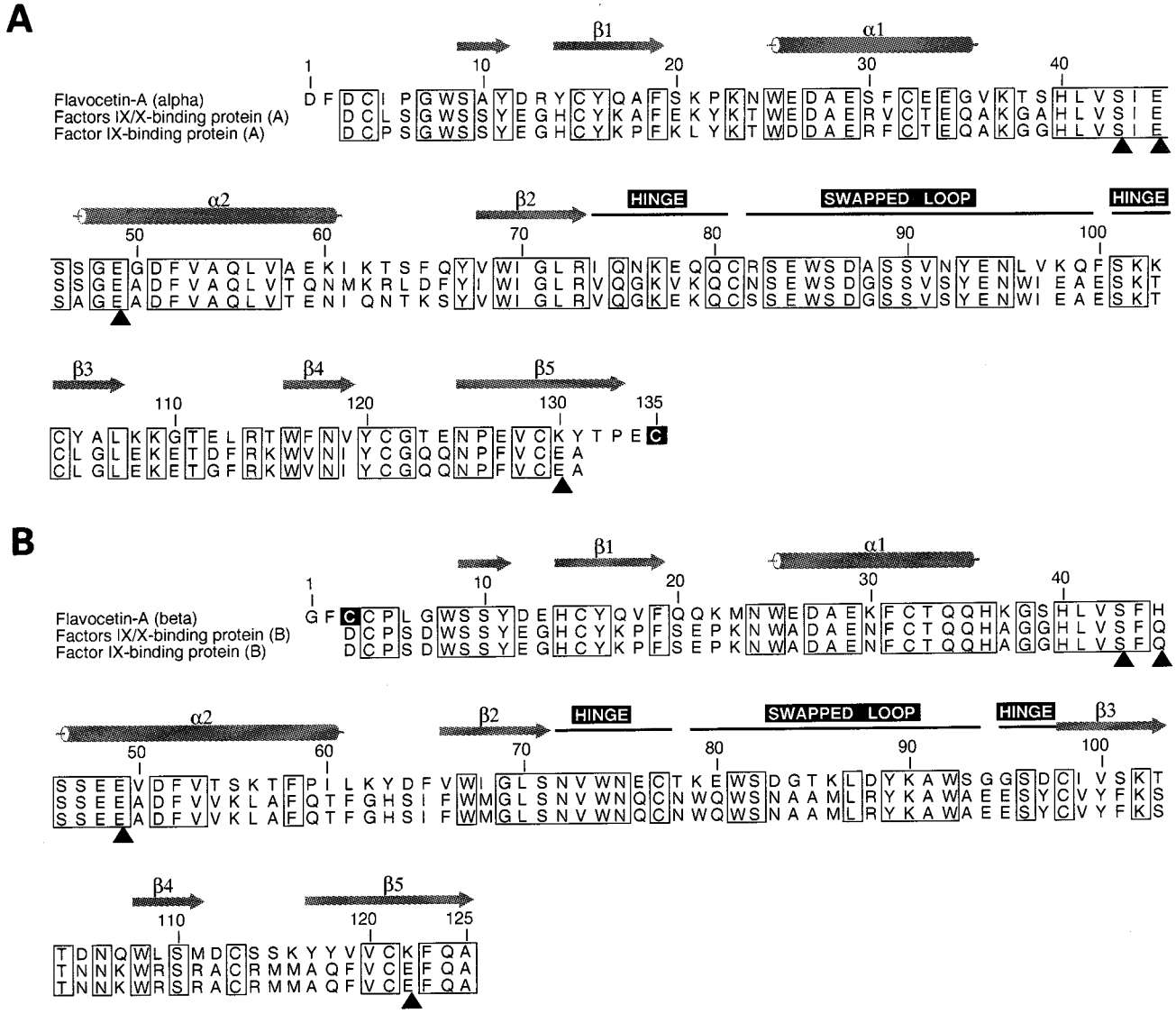

FIGURE 1: Structure-based sequence alignment of the C-type lectin-like proteins from snake venom. (A) Sequence alignment of the α-subunit of flavocetin-A (FL-A) from the *Trimeresurus flavoviridis* venom with the A-subunits of coagulation factors IX/X-binding protein (IX/X-bp) and coagulation factor IX-binding protein (IX-bp) both from the *T. flavoviridis* venom. The numbering and the secondary structural elements refer to the sequence of the subunit of FL-A. The α-helices and the *β*-strands of each subunit are indicated as cylinders and arrows, respectively. Identical residues are boxed. The sequence identities of the α-subunit of FL-A with the A-subunits of IX/X-bp and IX-bp are both 55.6%. The cysteine residue for interchain disulfide bridge for tetramerization is highlighted. The residues for calcium-binding sites in IX/X-bp and IX-bp are indicated by triangles. Swapped loop and hinge regions are indicated. (B) Sequence alignment of the *β*-subunit of FL-A with the B-subunits of IX/X-bp and IX-bp. The sequence identities of the *β*-subunit of FL-A with the B-subunits of IX/X-bp and IX-bp are both 50.4%. This figure was generated using the program ALSCRIPT (*54*).

ing, individual *B*-factor, and positional refinement protocols in the X-PLOR package in the resolution range between 6.0 and 2.5 Å. The *R*-factor and R_{free} improved to 21.8% and 27.8%, respectively; 93 water molecules were added in the model using the X-SOLVATE subroutine of QUANTA. Criteria for the inclusion of water molecules in the structure were the appearance of peaks at 1σ in ($2F_o-F_c$) maps and 3σ in (F_o-F_c) maps, and at least one hydrogen bonding interaction with the protein. The final refined model had the *R*-factor of 21.0% (23.1%) and R_{free} of 26.9% (28.6%) against data with 2σ cutoff (without σ cutoff) in the resolution range between 6.0 and 2.5 Å. The root-mean-square (rms) deviations from ideal bond lengths and angles were 0.007 Å and 1.6°, respectively. The average *B*-factors for protein and waters were 35.2 and 54.7 Å^2, respectively. Table 1 shows a summary of the data collection and refinement statistics. The stereochemistry of the final model was examined by the program PROCHECK (*43*). The most favored region in the Ramachandran plot (*44*) contains 81% of the number of nonglycine and nonproline residues. There are only two residues (Lysα37 and Asp*β*12) in the disallowed region in the Ramachandran plot. The solvent accessible surface area was calculated using the PROTEIN PACKAGE option in the program QUANTA using a 1.4 Å radius of the probe (water molecule).

RESULTS AND DISCUSSION

Overall Structure. Crystals of FL-A show the tetragonal space group *I* 4 with one α*β*-heterodimer per asymmetric unit (*34*). The backbone chain fold of the α*β*-heterodimer is almost identical to those of the homologous proteins, IX/X-bp and coagulation factor IX-binding protein (IX-bp), from the venom of *T. flavoviridis* as expected from high sequence identity (Figure 1). The α- and *β*-subunits are dimerized in

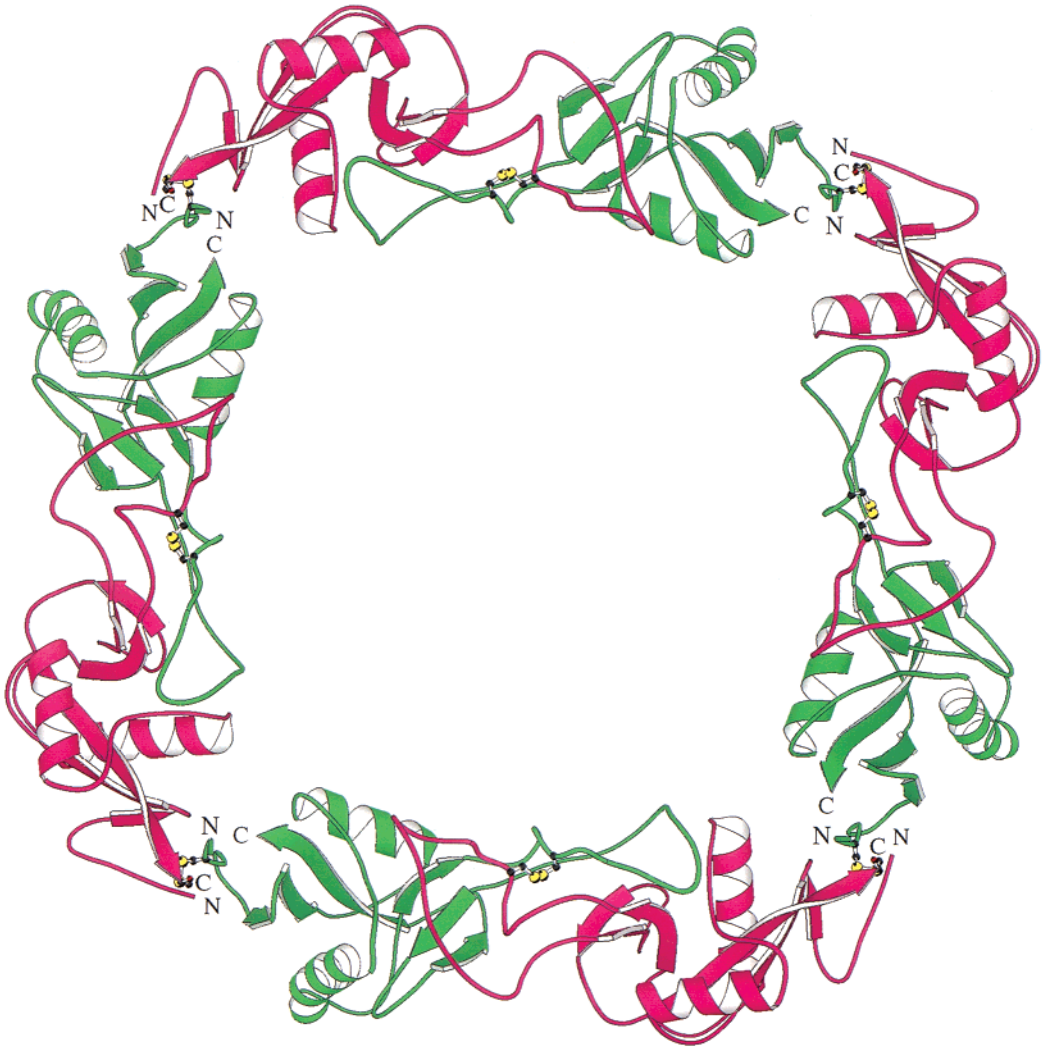

FIGURE 2: Ribbon drawing of the FL-A tetramer. The FL-A molecule is viewed down the crystallographic 4-fold axis. The α- and *β*-subunits are shown in magenta and green, respectively. The interchain disulfide bridges within and between the α*β*-heterodimers are shown in ball-and-stick representations. Carbon and sulfate atoms of the disulfide bridges are shown in black and yellow, respectively. N- and C-terminals of each subunit are labeled. This figure was generated using the program MOLSCRIPT (*55*).

a manner similar to 3D domain swapping (*45*) as already described in IX/X-bp and IX-bp (*39*, *46*), and an interchain disulfide bridge connects the two subunits. The overall structure of FL-A is made up of four α*β*-heterodimers related by a crystallographic 4-fold symmetry parallel to the *c*-axis, showing a cyclic tetramer $(\alpha\beta)_4$. The tetramerization is mediated by another interchain disulfide bridge newly identified between cysteine residues at the C-terminus of the α-subunit and at the N-terminus of the *β*-subunit of the neighboring α*β*-heterodimer. FL-A is thus a high-molecular mass protein (149 kDa) with a unique cyclic oligomer structure through the disulfide covalent interaction (Figure 2). The α*β*-heterodimers are arranged in a manner of "head-to-tail" interaction between cysteine residues located at either end of the long axis of the almost linearly elongated dimer unit, forming a square flat ring with dimensions approximately $126 \times 126 \times 37$ Å^3 with the disulfide bridge at each corner. The accessible surface area of the molecule was 47 907 Å^2. The unusual cyclic square molecule delimits a central pore with approximately $66 \times 66 \times 37$ Å^3, providing an extensive solvent channel that is consistent with the relatively large solvent content of 67% in the crystal.

Comparison with Other C-Type Lectin-like Heterodimers. FL-A is the first published structure comprising multiple copies of C-type lectin-like heterodimers. Known structures of IX/X-bp and IX-bp derived from the venom of *T. flavoviridis* are made up of only one C-type lectin-like heterodimer. A structural comparison between FL-A and IX/X-bp (hereafter, only IX/X-bp is used for comparison with FL-A because the structure of IX-bp is very similar to that of IX/X-bp) showed that the rms difference for the equivalent 99(97) C_α atom pairs except for the central loops between the α (*β*)-subunit of FL-A and the A (B)-subunit of IX/X-bp is 0.97 Å (0.81 Å). While, the rms difference for the equivalent 19(18) C_α atom pairs of the corresponding central loops between the α (*β*)-subunit of FL-A and the A (B)-subunit of IX/X-bp is 0.73 Å (0.86 Å). In contrast with such structural similarity, the relative disposition of the α- and *β*-subunits of FL-A is different from that of the A- and B-subunits of IX/X-bp; i.e., when the *β*- and B-subunits are superimposed, the α-subunit deviates significantly from the position of the A-subunit (Figure 3). Approximately, a 10° rotation of the α-subunit relative to the *β*-subunit is required for the superposition. This angle is larger than the corre-

FIGURE 3: Stereoviews of the C_α trace of the $\alpha\beta$-heterodimer of FL-A and the superposition onto IX/X-bp. (A) Stereoview of the C_α trace of the $\alpha\beta$-heterodimer of FL-A with every twentieth residue numbered. The α- and β-subunits are colored in magenta and green, respectively. (B) Stereoview of the superposition of the $\alpha\beta$-heterodimer of FL-A (magenta), in the same view as A, onto IX/X-bp (blue). The superposition was calculated with the equivalent 97 C_α atom pairs between the β-subunit of FL-A and the B-subunit of IX/X-bp. This figure was generated using the program MOLSCRIPT (*55*).

sponding value (6° rotation) in the cases of IX/X-bp and IX-bp, and forms a more opened concave surface. This is generated from a constraint by the interchain disulfide bridge between the $\alpha\beta$-heterodimers for tetramerization in FL-A.

Another structural difference between FL-A and IX/X-bp is whether or not calcium-binding sites are present. IX/X-bp has two common calcium-binding sites; one is in the A-subunit and the other in the homologous site of the B-subunit. In contrast, these potential sites in FL-A are not present despite being topologically equivalent to those in IX/X-bp. This is due to differences in amino acid residues. The residues Ser41, Glu43, and Glu47 in the calcium-binding site of the A-subunit in IX/X-bp are conserved, but the residue Glu128 is replaced by lysine at the corresponding site in the α-subunit of FL-A. Figure 4 shows the differences in these sites between the corresponding subunits in both FL-A and IX/X-bp. The residue Lysα130 is inserted into the site corresponding to the position of the calcium ion in the A-subunit of IX/X-bp. The atom NZ of Lysα130 replaces the calcium ion (Figure 4A) and forms the hydrogen bonds with the atom OE2 of Gluα45 (2.72 Å) and the atom OE1 of Gluα49 (2.86 Å). Similarly, the residues Ser41 and Glu47 in the calcium-binding site of the B-subunit in IX/X-bp are conserved, but the residues Gln43 and Glu120 are replaced by histidine and lysine, respectively, in the corresponding site in the β-subunit of FL-A. The atom NZ of Lysβ122 replaces the calcium ion (Figure 4B) and forms the hydrogen bonds with the backbone oxygen of Serβ43 (3.21 Å), the atom OE2 of Gluβ49 (3.01 Å), the oxygen of Wat27 (hereafter, a water molecule is referred to as a Wat)

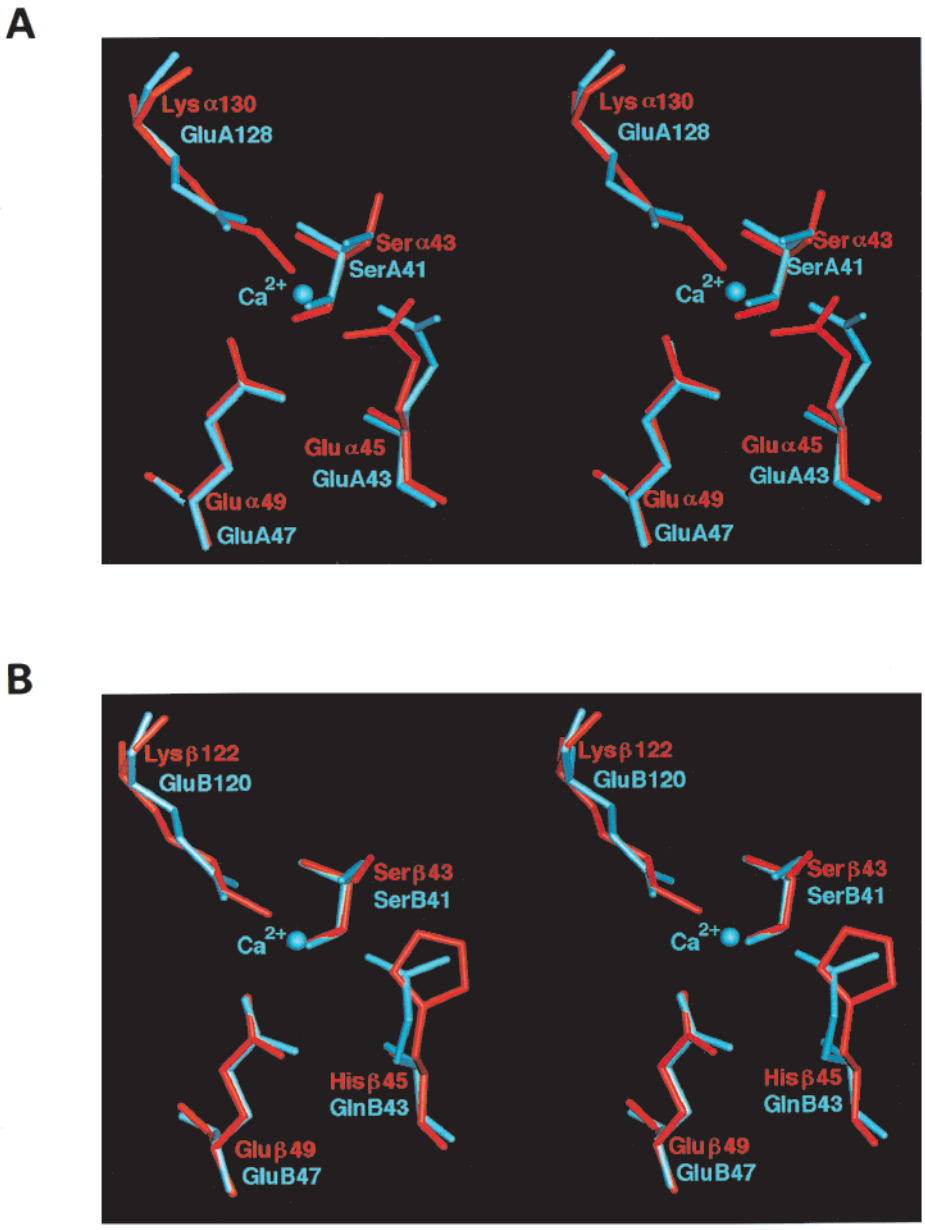

FIGURE 4: Comparison of the calcium-binding sites of IX/X-bp with the equivalent regions of FL-A. (A) Stereoview of superposition of the calcium-binding site of the A-subunit of IX/X-bp and the equivalent region of the α-subunit of FL-A. FL-A and IX/X-bp are colored in red and blue, respectively. Calcium ions are shown in blue spheres. (B) Stereoview of superposition of the calcium-binding site of the B-subunit of IX/X-bp and the equivalent region of the *β*-subunit of FL-A. This figure was generated using QUANTA.

(3.26 Å), and the atom OG of Ser*β*43 (3.02 Å). These hydrogen bonds and the neutralization by positively charged lysine residues may stabilize the structure of FL-A without calcium-binding.

Intersubunit Interfaces. There are two types of an intersubunit interface in the molecule of FL-A within and between the α*β*-heterodimers. One is an interface within the α*β*-heterodimer generated from a domain swapping. This interface corresponds to the C-interface defined in 3D domain swapping (*45*). This C-interface in FL-A is represented by a hydrophobic interaction between the central loop of one subunit and a body side in the globular unit of the adjacent subunit as described in IX/X-bp (*39*) and IX-bp (*46*). The residues involved in the C-interface in FL-A are as follows: the residues Trp81 (Trp85), Leu87 (Val91), Tyr89 (Tyr93), and Trp92 (Leu96) in the swapped loop of the *β*(α)-subunit and the residues Ile44 (Phe44), Leu72 (Leu70), and Trp116 (Trp108) on the body side of the α(*β*)-subunit. Although the residue corresponding to Trp77 in the swapped loop of the B-subunit in IX/X-bp (*38*) is replaced by Lys79 (Ser83) in the swapped loop of the *β*(α)-subunit in FL-A, this is similar to the case of the residue Ser81 in the swapped loop of the A-subunit in IX/X-bp. The two subunits are held together by a common interchain disulfide bridge between the residues Cysα81 and Cys*β*77. Recently, sequenced C-type lectin-like heterodimer protein rhodocetin, a platelet aggregation inhibitor isolated from the venom of the Malayan pit viper *Calloselasma rhodostoma*, has no such interchain disulfide bridge (*47*). The α- and *β*-subunits in this protein are held together only by noncovalent interactions, probably the C-interface, because it is expected to be a domain-swapped heterodimer. The C-interface in the C-type lectin-like heterodimer from snake venom is thus crucial to connect the subunits.

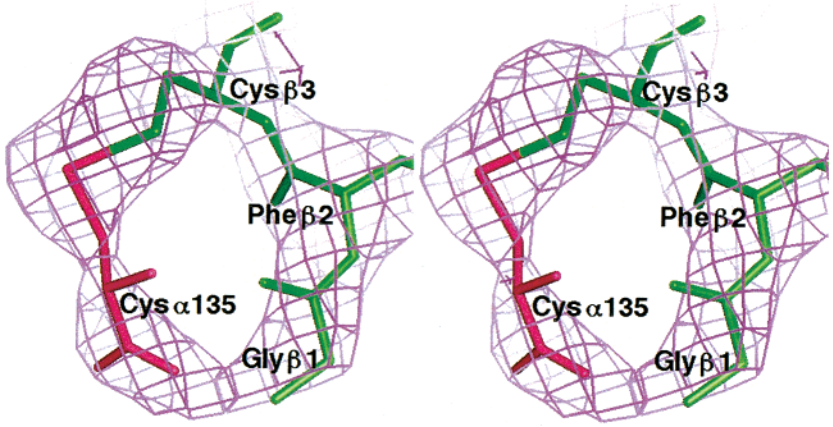

FIGURE 5: Stereoview of the electron-density map ($2F_o - F_c$ map, contoured at 1σ) around the interchain disulfide bridge between the $\alpha\beta$-heterodimers. The residues Cysα135 in the α-subunit (magenta) and Glyβ1-Cysβ3 in the β-subunit (green) of the neighboring $\alpha\beta$-heterodimer are labeled. This figure was generated using QUANTA.

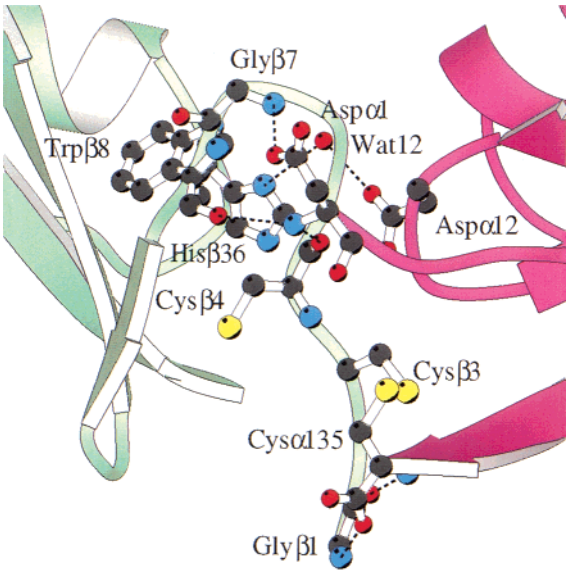

FIGURE 6: A close-up view of the tetramerization interface. Residues and one water molecule involving hydrogen bonds between the α(magenta)- and β(green)-subunits are shown in ball-and-stick representations. Carbon, oxygen, and nitrogen atoms are colored in black, red, and blue, respectively. This figure was generated using the program MOLSCRIPT (*55*).

Table 2: Interactions Between the α- and β-Subunits Found at the Tetramer Interface

type of interactions	α-subunit	β-subunit
disulfide bridge	Cys135	Cys3
hydrogen bonds	Cys135-OT	Gly1-N (2.42)[a]
	Cys135-N	Gly1-O (2.80)
	Asp1-N	Trp8-O (3.03)
	Asp1-N	Cys4-O (2.95)
	Asp1-OD1	Gly7-N (2.95)
water-mediated (Wat12)	Asp12-OD1 (2.69)	His36-ND1 (2.81)

[a] Hydrogen bond distances (Å) are indicated.

Another subunit interface is formed between the $\alpha\beta$-heterodimers where the α- and β-subunits are connected by another disulfide bridge between the residues Cysα135 and Cysβ3, lying in the C-terminal β-strand of the α-subunit and the N-terminal loop of the β-subunit, respectively. The electron-density map around the disulfide bridge is shown in Figure 5. The residue Cysα135 is at the end of the additional C-terminal peptide, which is largely exposed from the body compared with IX/X-bp (Figure 3B), allowing the disulfide bridge with the residue Cysβ3 that replaces aspartic acid in IX/X-bp. Five direct hydrogen bonds and one water-mediated hydrogen bond exist in this interface (Figure 6, Table 2). Involved in the hydrogen bonds are mainly the backbone chain nitrogen and oxygen atoms and three side chains of the residues Asp1-OD1 and Asp12-OD1 in the α-subunit, and His36-ND1 in the β-subunit of the neighboring $\alpha\beta$-heterodimer. The buried area is 400 Å^2. This corresponds to 3.1% of the total accessible surface area (12 777 Å^2) of one $\alpha\beta$-heterodimer, well below the value for typical oligomeric proteins (*48*). This contact area is so small that the interchain disulfide bridge may play a central role to form and stabilize the tetrameric heterodimer structure of FL-A.

Platelet GP Ib-Binding. FL-A binds with high affinity to the platelet GP Ib α-subunit and functions as a strong inhibitor of vWF-dependent aggregation of fixed human platelets (*33*). It has been reported that FL-A has a dissociation constant of 0.35 ± 0.13 nM to platelets, according to the results of a direct-binding assay using iodine-labeled FL-A and fixed human platelets (*33*), showing approximately 10- to 100-fold less than the value of echicetin from the *Echis carinatus* venom (*21*). Convulxin (CVX), another high-molecular mass C-type lectin-like protein (72 kDa) from the *Crotalus durissus terrificus* venom (*49*), binds with high affinity (K_d = 30 pM) to the collagen receptor GP VI and functions as a very potent inducer of platelet aggregation (*50*−*52*). These facts reflect that the oligomer proteins comprise multiple copies of the $\alpha\beta$-heterodimer and induce the binding to the platelet GP receptors more efficiently than proteins made up of only one $\alpha\beta$-heterodimer. CVX has also additional cysteine residues, Cysα135 and Cysβ3, which might form an interchain disulfide bridge for oligomerization as observed in FL-A. Leduc and Bon postulated that CVX is a trimer $(\alpha\beta)_3$ of the $\alpha\beta$-heterodimers (*53*), although there is no structural evidence to support this. The residues in FL-A involved in the intersubunit interface, which are important for the tetramerization as described above, are well-conserved in CVX. This suggests that the $\alpha\beta$-heterodimers of CVX are arranged in a manner similar to FL-A to form a cyclic oligomer. Such oligomerization of the $\alpha\beta$-heterodimers might

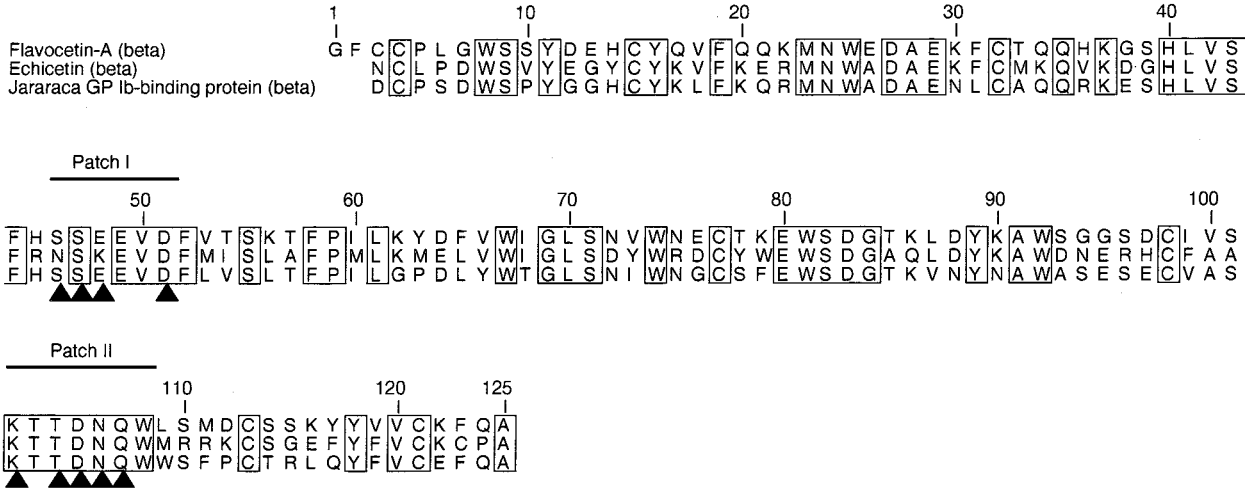

FIGURE 7: Sequence alignment of the β-subunit of FL-A with the β-subunits of other GP Ib-binding proteins from snake venom, echicetin from the *Echis carinatus* venom, and jararaca GP Ib-binding protein from the *Bothrops jararaca* venom. The numbering refers to the sequence of the β-subunit of FL-A. The conserved residues are boxed. The sequence identities are 54.4% (echicetin) and 60.8% (jararaca GP Ib-binding protein). The residues involved in putative GP Ib-binding are shown by two hydrophilic patches marked by lines above the alignment where triangles below the alignment show solvent-exposed residues. This figure was generated using the program ALSCRIPT (*54*).

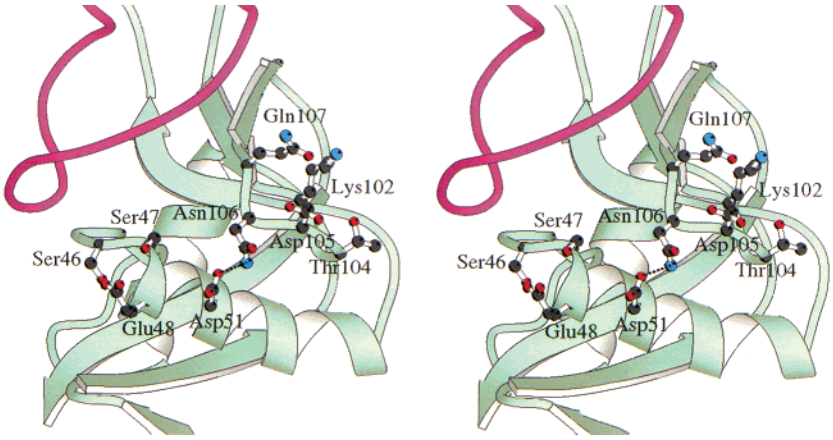

FIGURE 8: Stereo-ribbon drawing around the putative GP Ib-binding sites of FL-A. Main chains in the α- and β-subunits are shown in magenta and green, respectively. The solvent-exposed residues in the hydrophilic patches are indicated by ball-and-stick representations. Carbon, oxygen, and nitrogen atoms are colored in black, red, and blue, respectively. This figure was generated using the program MOLSCRIPT (*55*).

generate a cooperative-binding action through the multiple binding sites to platelet GP receptor to gain a much higher affinity.

The high-sequence identities with other GP Ib-binding proteins, i.e., echicetin from the *E. carinatus* venom (*27*, *30*) and jararaca GP Ib-binding protein from the *B. jararaca* venom (*28*) (Figure 7, only the β-subunits are compared because of hydrophilic patches described below), imply that their three-dimensional structures are very similar to that of the $\alpha\beta$-heterodimer of FL-A. Although the conserved peptides mapped on the sequence are mainly involved in the formation of hydrophobic cores inside the $\alpha\beta$-heterodimer, two peptide fragments in the β-subunit show hydrophilic patches exposed to solvent (Figures 7 and 8), which are considered as possible candidates for the platelet GP Ib-binding sites. One is in the second α-helix in the β-subunit where the residues Serβ46, Serβ47, Gluβ48, and Aspβ51 (Asnβ44 and Lysβ46 in echicetin) are involved (patch I). This patch is in a slightly deeper pocket near the central concave surface of the $\alpha\beta$-heterodimer. Another hydrophilic patch (patch II) is formed by the residues Lysβ102, Thrβ104, Aspβ105, Asnβ106, and Glnβ107, which lie in a loop closed by an intrachain disulfide bond between the residues Cysβ98 and Cysβ113. So the backbone chain position is relatively constrained and contributes to the formation of a part of the central concave surface of the $\alpha\beta$-heterodimer. The atom ND2 of the residue Asnβ106 in the patch II forms a salt bridge (2.90 Å) with the atom OD1 of the residue Aspβ51 in the patch I, showing these patches are spatially close together (Figure 8). The candidates for the platelet GP Ib α-binding sites are thus in the β-subunit, but not in the α-subunit. This is consistent with the result of an inhibition study based on an enzyme-linked immunosorbent assay using biotin-labeled jararaca GP Ib-binding protein from the *B. jararaca* venom and competing ligands (*28*). Crystallographic studies of FL-A in complex with the platelet GP Ib α-subunit are required to know the binding sites and the interactions between the two molecules.

The crystal structure of FL-A at 2.5 Å resolution revealed that FL-A is a novel cyclic tetramer $(\alpha\beta)_4$ made up of four identical C-type lectin-like $\alpha\beta$-heterodimers covalently held together by interchain disulfide bridges. This study also

revealed for the first time a three-dimensional structure of the platelet GP Ib-binding protein. The high affinity of FL-A for the platelet GP Ib α-subunit could be explained by a cooperative-binding action through the multiple binding sites of the tetramer. The candidate of the binding sites is considered to be located along two hydrophilic patches on the β-subunit. The structure of FL-A presented here should constitute an essential background for the design and development of drugs and/or model compounds as platelet antagonists.

ACKNOWLEDGMENT

This work was performed with the approval of the Photon Factory Advisory Committee, High Energy Accelerator Research Organization, Tsukuba, Japan (proposal number 98G156). We gratefully acknowledge Drs. Noriyoshi Sakabe, Nobuhisa Watanabe, Mamoru Suzuki, and Noriyuki Igarashi for the use of the Weissenberg camera at the Photon Factory. We also gratefully acknowledge Dr. Yongchol Shin for performing the sequence analysis of FL-A.

REFERENCES

1. Ware, J. (1998) *Thromb. Haemostasis 79*, 466−478.
2. López, J. A., Andrews, R. K., Afshar-Kharghan, V., and Berndt, M. C. (1998) *Blood 91*, 4397−4418.
3. López, J. A. (1994) *Blood Coaguluation & Fibrinolysis 5*, 97−119.
4. Andrews, R. K., López, J. A., and Berndt, M. C. (1997) *Int. J. Biochem. Cell Biol. 29*, 91−105.
5. Ruggeri, Z. M. (1993) *Thromb. Haemostasis 70*, 119−123.
6. Kroll, M. H., Hellums, J. D., McIntire L. V., Schafer, A. I., and Moake, J. L. (1996) *Blood 88*, 1525−1541.
7. Tsuji, S., Sugimoto, M., Kuwahara, M., Nishio, K., Takahashi, Y., Fujimura, Y., Ikeda, Y., and Yoshioka, A. (1996) *Blood 88*, 3854−3861.
8. Markland, F. S. (1998) *Toxicon 36*, 1749−1800.
9. Read, M. S., Schermer, R. W., and Brinkhous, K. M. (1978) *Proc. Natl. Acad. Sci. U.S.A. 75*, 4514−4518.
10. Brinkhous, K. M., Read, M. S., Fricke, W. A., and Wagner, R. H. (1983) *Proc. Natl. Acad. Sci. U.S.A. 80*, 1463−1466.
11. Andrews, R. K., Booth, W. J., Gorman, J. J., Castaldi, P. A., and Berndt, M. C. (1989) *Biochemistry 28*, 8317−8326.
12. Fujimura, Y., Titani K., Usami, Y., Suzuki, M., Oyama, R., Matsui, T., Fukui, H., Sugimoto, M., and Ruggeri, Z. M. (1991) *Biochemistry 30*, 1957−1964.
13. Usami, Y., Fujimura, Y., Suzuki, M., Ozeki, Y., Nishio, K., Fukui, H., and Titani, K. (1993) *Proc. Natl. Acad. Sci. U.S.A. 90*, 928−932.
14. Read, M. S., Smith, S. V., Lamb, M. A., and Brinkhous, K. M. (1989) *Blood 74*, 1031−1035.
15. Sugimoto, M., Mohri, H., McClintock, R. A., and Ruggeri, Z. M. (1991) *J. Biol. Chem. 266*, 18172−18178.
16. Hamako, J., Matsui, T., Suzuki, M., Ito, M., Makita, K., Fujimura, Y., Ozeki, Y., and Titani, K. (1996) *Biochem. Biophys. Res. Commun. 226*, 273−279.
17. Matsui, T., Hamako, J., Suzuki, M., Hayashi, N., Ito, M., Makita, K., Fujimura, Y., Ozeki, Y., and Titani, K. (1997) *Res. Commun. Biochem. Cell Mol. Biol. 1*, 271−284.
18. Obert, B., Houllier, A., Meyer, D., and Girma, J.-P. (1999) *Blood 93*, 1959−1968.
19. Peng, M., Lu, W., and Kirby, E. P. (1991) *Biochemistry 30*, 11529−11536.
20. Peng, M., Lu, W., and Kirby, E. P. (1992) *Thromb. Haemostasis 67*, 702−707.
21. Peng, M., Lu, W., Beviglia, L., Niewiarowski, S., and Kirby, E. P. (1993) *Blood 81*, 2321−2328.
22. Kawasaki, T., Taniuchi, Y., Hisamichi, N., Fujimura, Y., Suzuki, M., Titani, K., Sakai, Y., Kaku, S., Satoh, N., Takenaka, T., Handa, M., and Sawai, Y. (1995) *Biochem. J. 308*, 947−953.
23. Fujimura, Y., Ikeda, Y., Miura, S., Yoshida, E., Shima, H., Nishida, S., Suzuki, M., Titani, K., Taniuchi, Y., and Kawasaki, T. (1995) *Thromb. Haemostasis 74*, 743−750.
24. Chen, Y.-L., and Tsai, I.-H. (1995) *Biochem. Biophys. Res. Commun. 210*, 472−477.
25. Andrews, R. K., Kroll, M. H., Ward, C. M., Rose, J. W., Scarborough, R. M., Smith, A. I., López, J. A., and Berndt, M. C. (1996) *Biochemistry 35*, 12629−12639.
26. Sakurai, Y., Fujimura, Y., Kokubo, T., Imamura, K., Kawasaki, T., Handa, M., Suzuki, M., Matsui, T., Titani, K., and Yoshioka, A. (1998) *Thromb. Haemostasis 79*, 1199−1207.
27. Peng, M., Holt, J. C., and Niewiarowski, S. (1994) *Biochem. Biophys. Res. Commun. 205*, 68−72.
28. Kawasaki, T., Fujimura, Y., Usami, Y., Suzuki, M., Miura, S., Sakurai, Y., Makita, K., Taniuchi, Y., Hirano, K., and Titani, K. (1996) *J. Biol. Chem. 271*, 10635−10639.
29. Usami, Y., Suzuki, M., Yoshida, E., Sakurai, Y., Hirano, K., Kawasaki, T., Fujimura, Y., and Titani, K. (1996) *Biochem. Biophys. Res. Commun. 219*, 727−733.
30. Polgár, J., Magnenat, E. M., Peitsch, M. C., Wells, T. N. C., Saqi, M. S. A., and Clemetson, K. J. (1997) *Biochem. J. 323*, 533−537.
31. Fujimura, Y., Kawasaki, T., and Titani, K. (1996) *Thromb. Haemostasis 76*, 633−639.
32. Drickamer, K. (1993) *Prog. Nucleic Acid Res. Mol. Biol. 45*, 207−232.
33. Taniuchi, Y., Kawasaki, T., Fujimura, Y., Suzuki, M., Titani, K., Sakai, Y., Kaku, S., Hisamichi, N., Satoh, N., Takenaka, T., Handa, M., and Sawai, Y. (1995) *Biochim. Biophys. Acta 1244*, 331−338.
34. Fukuda, K., Mizuno, H., Atoda, H., and Morita, T. (1999) *Acta Crystallogr. D55*, 1911−1913.
35. Sakabe, N. (1991) *Nucl. Instrum. Methods Phys. Res., Sect. A 303*, 448−463.
36. Otwinowski, Z., and Minor, W. (1997) *Methods Enzymol. 276*, 307−326.
37. Navaza, J. (1994) *Acta Crystallogr. A50*, 157−163.
38. Collaborative Computational Project, Number 4. (1994) *Acta Crystallogr. D50*, 760−763.
39. Mizuno, H., Fujimoto, Z., Koizumi, M., Kano, H., Atoda, H., and Morita, T. (1997) *Nat. Struct. Biol. 4*, 438−441.
40. Brünger, A. T. (1992) *X-PLOR Manual, version 3.1.*, Yale University, New Haven, CT.
41. Engh, R. A., and Huber, R. (1991) *Acta Crystallogr. A47*, 392−400.
42. Brünger, A. T. (1997) *Methods Enzymol. 277*, 366−396.
43. Laskowski, R. A., MacArthur, M. W., Moss, D. S., and Thornton, J. M. (1993) *J. Appl. Crystallogr. 26*, 283−291.
44. Ramachandran, G. N., and Sasisekharan, V. (1965) *Adv. Protein Chem. 23*, 283−437.
45. Bennett, M. J., Schlunegger, M. P., and Eisenberg, D. (1995) *Protein Sci. 4*, 2455−2468.
46. Mizuno, H., Fujimoto, Z., Koizumi, M., Kano, H., Atoda, H., and Morita, T. (1999) *J. Mol. Biol. 289*, 103−112.
47. Wang, R., Kini, R. M., and Chung, M. C. M. (1999) *Biochemistry 38*, 7584−7593.
48. Janin, J., Miller, S., and Chothia, C. (1988) *J. Mol. Biol. 204*, 155−164.
49. Prado-Franceschi, J., and Brazil, O. V. (1981) *Toxicon 19*, 875−887.
50. Francischetti, I. M. B., Saliou, B., Leduc, M., Carlini, C. R., Hatmi, M., Randon, J., Faili, A., and Bon, C. (1997) *Toxicon 35*, 1217−1228.
51. Polgár, J., Clemetson, J. M., Kehrel, B. E., Wiedemann, M., Magnenat, E. M., Wells, T. N. C., and Clemetson, K. J. (1997) *J. Biol. Chem. 272*, 13576−13583.
52. Jandrot-Perrus, M., Lagrue, A.-H., Okuma, M., and Bon, C. (1997) *J. Biol. Chem. 272*, 27035−27041.
53. Leduc, M., and Bon, C. (1998) *Biochem. J. 333*, 389−393.
54. Barton, G. J. (1993) *Protein Eng. 6*, 37−40.
55. Kraulis, P. J. (1991) *J. Appl. Crystallogr. 24*, 946−950.

BI992134Z